HMG Advance Access published February 2, 2010

Human Molecular Genetics, 2010 **1–8**
doi:10.1093/hmg/ddq019

A milieu of regulatory elements in the epidermal differentiation complex syntenic block: implications for atopic dermatitis and psoriasis

Cristina de Guzman Strong[1], Sean Conlan[1], Clayton B. Deming[1], Jun Cheng[1], Karen E. Sears[2] and Julia A. Segre[1,*]

[1]Genetics and Molecular Biology Branch, National Human Genome Research Institute, NIH, Bethesda, MD, USA and [2]Department of Animal Biology, University of Illinois, Urbana, IL, USA

Received November 2, 2009; Revised December 28, 2009; Accepted January 18, 2010

Two common inflammatory skin disorders with impaired barrier, atopic dermatitis (AD) and psoriasis, share distinct genetic linkage to the Epidermal Differentiation Complex (EDC) locus on 1q21. The EDC is comprised of tandemly arrayed gene families encoding proteins involved in skin cell differentiation. Discovery of semi-dominant mutations in filaggrin (*FLG*) associated with AD and a copy number variation within the *LCE* genes associated with psoriasis provide compelling evidence for the role of EDC genes in the pathogenesis of these diseases. To date, little is known about the potentially complex regulatory landscape within the EDC. Here, we report a computational approach to identify conserved non-coding elements (CNEs) in the EDC queried for regulatory function. Coordinate expression of EDC genes during mouse embryonic skin development and a striking degree of synteny and linearity in the EDC locus across a wide range of mammalian (placental and marsupial) genomes suggests an evolutionary conserved regulatory milieu in the EDC. CNEs identified by comparative genomics exhibit dynamic regulatory activity (enhancer or repressor) in differentiating or proliferating conditions. We further demonstrate epidermal-specific, developmental *in vivo* enhancer activities (DNaseI and transgenic mouse assays) in CNEs, including one within the psoriasis-associated deletion, *LCE3C_LCE3B-del*. Together, our multidisciplinary study features a network of regulatory elements coordinating developmental EDC gene expression as an unexplored resource for genetic variants in skin diseases.

INTRODUCTION

The Epidermal Differentiation Complex (EDC) spanning 1.6 Mb on human 1q21 (mouse 3q) harbors four clusters of tandem gene families: Filaggrin (*FLG*)-like, Late Cornified Envelope (*LCE*), Small Proline Rich Region (*SPRR)* and the *S100* genes (Fig. 1) (1–5). *FLG*-like, *LCE* and *SPRR* genes encode structural proteins which are cross-linked to form the essential epidermal barrier at the surface of the skin, although *S100* genes encode chemoattractant proteins expressed when the barrier is impaired (6). Recently, the EDC has been implicated in two common inflammatory skin disorders with impaired barrier, atopic dermatitis (AD) and psoriasis, that both share distinct genetic linkage to the EDC suggesting a role for these genes in disease pathogenesis (7–9). Loss-of-function variants in the *FLG* gene that were first identified in ichthyosis vulgaris, a common dry, scaly skin disorder (10), are also strongly associated with AD with subsequent progression to asthma or allergic rhinitis known as the atopic march (8,11,12). However, only 50% of AD patients possess *FLG* null alleles (12) and exclusion of the common *FLG* alleles in familial AD studies continues to demonstrate linkage to the EDC suggesting additional genetic variants in the *FLG*-like genes and the EDC (9,13). Recent genome-wide association studies identified association of psoriasis to a 30-kb deletion spanning the *LCE3C* and *LCE3B* genes (*LCE3C_LCE3B-del*) (14,15). Although psoriatic skin samples from *LCE3C_LCE3B-del* genotyped patients demonstrated a decrease in LCE3C and LCE3B expression, it is possible that a regulatory element within the *LCE3C_LCE3B-del* allele could be a contributing factor as well.

The spatial and temporal expression of several genes in the EDC during developmental epidermal differentiation and their dense tandem genomic arrangement suggest a genomic mechanism to coordinate their expression. One intriguing model for coordinate expression is a network of *cis*-regulatory

*To whom correspondence should be addressed. Tel: +1 3014022314; Fax: +1 3014024929; Email: jsegre@nhgri.nih.gov

Published by Oxford University Press 2010.

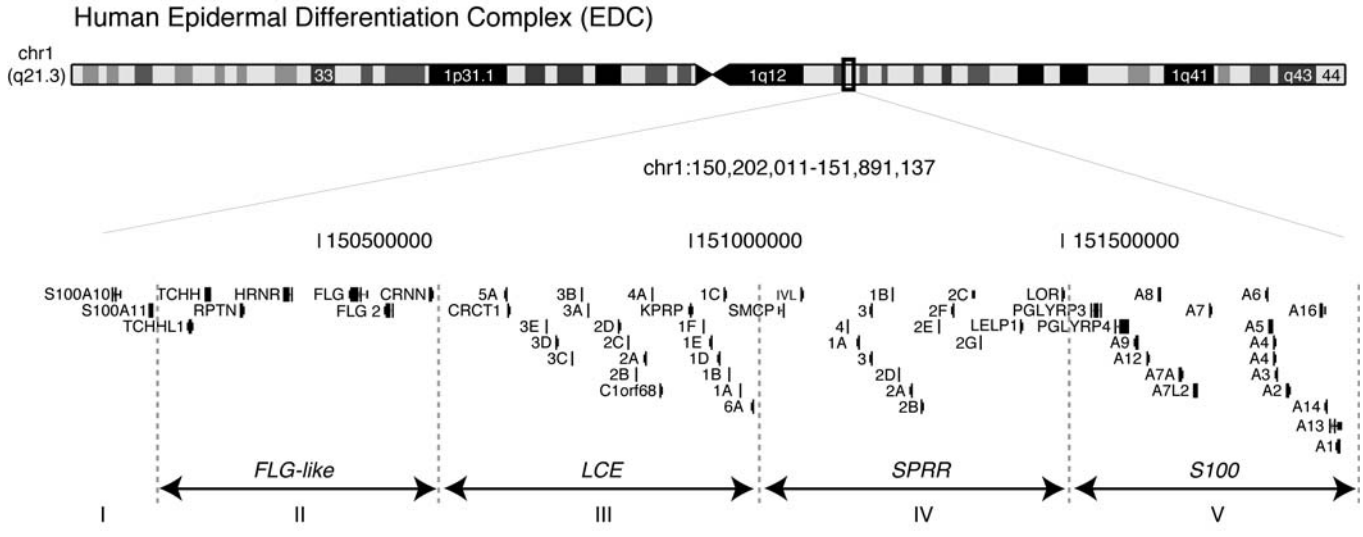

Figure 1. The EDC is comprised of tandemly arrayed gene families. Human (hg18) EDC on chromosome 1q21 (1.6 Mb).

elements in the EDC. Comparative genomics have greatly facilitated the identification of regulatory elements in Conserved Non-coding sequences or Elements (CNEs) (16). We apply this method to identify potential regulatory elements in the EDC locus as an untapped resource for functional genetics studies. Using this bioinformatics approach, we observe remarkable evolutionary conservation of the EDC locus across phylogenetically distinct mammalian genomes. Furthermore, we identified 48 CNEs in the EDC that exhibited dynamic regulatory activity during differentiating and proliferating conditions. We demonstrate epidermal-specific developmental *in vivo* enhancer activity in two CNEs, especially one in the psoriasis-associated *LCE3C_LCE3B-del* allele. These results highlight a genomic mechanism to coordinate developmental expression of the EDC genes via *cis*-regulatory elements that could likely play a role in human skin disease.

RESULTS

Developmental coordination of EDC gene expression during epidermal differentiation and skin barrier formation

To investigate the degree to which the EDC genes are coordinately regulated during skin epidermal development, we employed a semi-quantitative analysis of pan-EDC gene locus temporal expression in murine embryonic skin (Fig. 2A). In mice, epidermal differentiation commences at embryonic day (E)15.5 followed by acquisition of skin barrier formation at E16.5 (17). Our results indicate initial expression of a majority of the EDC genes (44/61) genes, at E15.5 compared with control E13.5 (Fig. 2B). By E16.5, 11 additional genes were induced, most notably the *LCE* genes as well as increased expression of other EDC genes. The *LCE* genes at the extreme 5′ and 3′ ends of the *LCE* gene family were induced at E15.5 followed by induction of the more internal *LCE* genes at E16.5. Although several of the *S100* genes demonstrated similar expression levels both at E15.5 and E16.5, not all *S100* genes were expressed suggesting a discrete mechanism of regulation. These data confirm and expand the previous *SPRR* and *LCE* gene family-centric analyses, which revealed cluster-specific gene expression in various adult human epithelia (18,19). Together, these data support a coordination of EDC temporal expression during epidermal development that can be facilitated by *cis*-regulatory elements.

The EDC represents an ultraconserved microsyntenic genomic block in mammals

To identify CNEs, we aligned orthologous EDC genes from multiple, phylogenetically distinct mammalian species: human, chimp, rhesus, mouse, rat, dog and opossum (Fig. 3). The metatherian (or marsupial) opossum, representing one of the furthest mammalian phylogenetic branches (diverged 180 million years ago from the human), provides unique insights in ascertaining mammalian biological processes in comparison to these mammals (20–22). For example, opossums exhibit the same patterning of epidermal barrier acquisition observed in other mammals (23,24) yet at an accelerated pace given the shortened gestational age *in utero* (~13 days) (Supplementary Material, Fig. 1). Given the observation of conserved patterning of epidermal barrier formation and its unique phylogenetic position in the mammalian lineage, we, therefore, incorporated the opossum genome to empower our comparative genomics studies. We find that the alignment of orthologous EDC genes in multiple mammalian species demonstrated a striking degree of linearity (order or arrangement of the genes) and synteny (genes occurring on the same chromosome) of orthologous EDC genes. Consistent with a shared genome-wide sequence identity to the human (93%) (25), the chimp and rhesus EDC loci are highly conserved (linear and syntenic). This conservation extended to the mammalian order *rodentia* where mouse and rat EDC loci differed from the human EDC locus in size (3.1 and 3.9 Mb, respectively) owing to a large

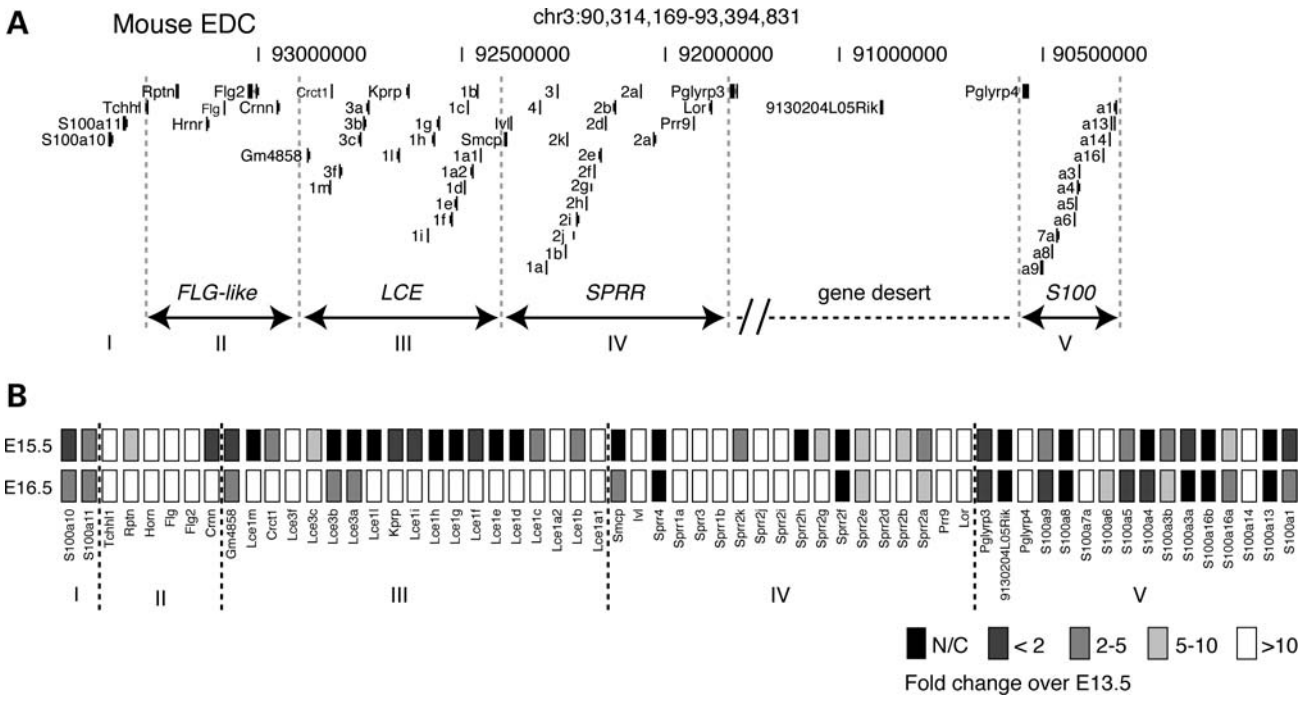

Figure 2. Coordinated expression of EDC genes during epidermal differentiation and barrier formation. (**A**) Mouse (mm9) EDC (chr3), 3.1 Mb, are comprised of 4 gene families (*FLG*-like [II], *LCE* [III], *SPRR* [IV] and *S100* [I and V]). Group I represents a cluster of 2 *S100* genes (*S100A10*, *S100A11*). (**B**) Heatmap reflecting a semiquantitative real-time PCR analysis of EDC gene expression from mouse dorsal skin at E15.5 (epidermal differentiation) and E16.5 (barrier formation). Experiments were done in triplicate ($n = 2$ per embryonic stage) and normalized to β_2-microglobulin. Gray scale legend, fold-change over E13.5 expression.

~1.3 Mb 'gene desert' insertion (telomeric to *HRN* and centromeric to the *FLG* genes). Analysis of orthologous genes in the opossum also revealed conserved linearity with a large 309 Mb insertion separating the *FLG*-like and *SPRR* gene families from the *LCE* and *S100* gene families (21). Analysis of the EDC orthologous genes in the dog revealed conserved linearity among the *FLG*-like, *LCE* and *SPRR* gene families with limited EDC synteny as the *S100* gene family mapped to another chromosome, suggesting independent regulation of the *S100* genes in the dog. Although the evolutionary time between the radiation of mammalian species is too short to produce the null hypothesis of randomly distributed genes in the genomes, the existence of orthologous EDC genes as linear and syntenic loci across mammalian genomes suggests a genetic mechanism to maintain the EDC as a regulatory block.

Regulatory activities in the CNEs of the EDC

In our search for regulatory elements, we identified 48 CNEs (range of 115–1403 bp; mean = 431 bp) using a conservative alignment of orthologous EDC loci from multiple mammalian species (Fig. 4A, Supplementary Material, Table S1, Methods). Totaling 19 847 bp, CNEs represent 1.2% of the human EDC, a majority of which are located intergenically. To determine the regulatory potential of the CNEs, we performed luciferase reporter assays on cultured epidermal cells (keratinocytes) under terminally differentiating and proliferating conditions (1.2 and 0.05 mM Ca^{2+}, respectively). Fourteen random Non-Conserved Non-coding Elements (NCNE) in the EDC (range of 115–1109 bp; mean = 496 bp) were used as a negative control. Nine CNEs exhibit enhancer activity (mean >2-fold increased luciferase activity) and six CNEs exhibit repressor activity (mean >2-fold decreased luciferase activity) under differentiating conditions (Fig. 4B). Under proliferating conditions, four CNE continued to demonstrate enhancer activity (Fig. 4C) and three CNE continued to demonstrate repressor activity. Three additional CNEs exhibited repressor activity exclusively under proliferating conditions. By comparison, all NCNE failed to exhibit enhancer or repressor activity (data not shown). In summary, these data demonstrate an enrichment of regulatory activity (30%, 15/48) of the EDC CNEs during differentiation compared with 20% (10/48) of the EDC CNEs during proliferation.

h923 and h621 in *LCE3C_LCE3B-del* function as epidermal-specific developmental enhancers *in vivo*

We further characterized the *in vivo* regulatory activity of two CNEs, selected either by *in vitro* enhancer activity or by disease relevance, using DNaseI hypersensitivity assays and transgenic mice. h923 is a 657-bp CNE located ~2.6 kb upstream of the involucrin (*IVL*) transcriptional start site and demonstrated the highest enhancer activity *in vitro*. h621 is a 333-bp CNE that maps within the psoriasis-associated *LCE3C_LCE3B-del* region. Regulatory elements, typically devoid of core nucleosome structure, are hypersensitive to DNaseI treatment (26). We quantified DNaseI sensitivity of human primary epidermal cells by real-time PCR and overlapping amplicons that tile across the targeted CNEs (27). *In vivo* tissue-specific enhancer activity was assayed using transgenic

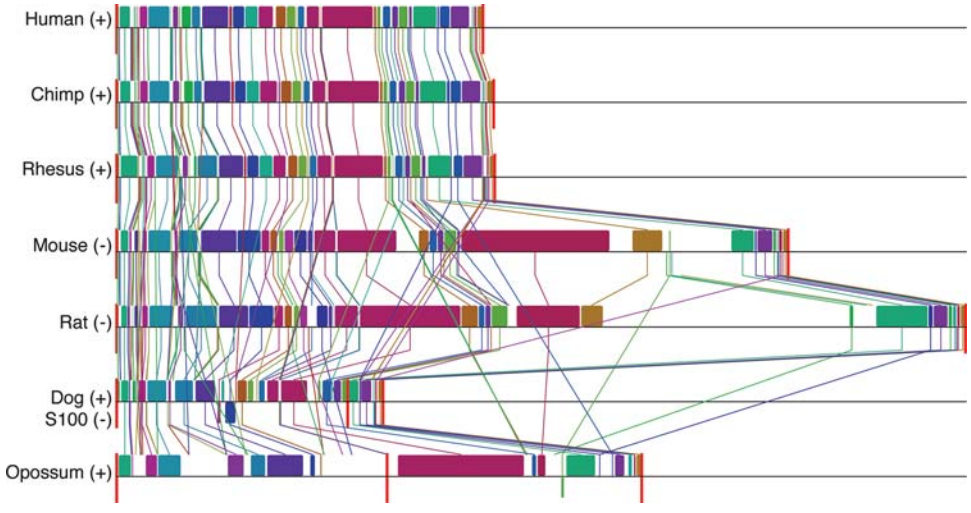

Figure 3. The EDC represents an ultraconserved microsyntenic block in mammals. Each EDC loci from human, chimp, rhesus, mouse, rat, dog and opossum is depicted as locally collinear blocks (LCBs) (colored boxes) representing homologous regions shared by the aligned genomes and does not contain any rearrangements. Vertical lines trace homologous LCBs between genomes. LCBs below a genome's center black line are in reverse complement orientation relative to the human reference EDC locus. Red vertical lines mark interchromosomal boundaries or chromosomal distances <100 000 kb (opossum). +, forward orientation; −, reverse complement. Note that the *S100* genes are in reverse complement in the dog.

CNE-*hsp68-lacZ* reporter mice that only demonstrate β-galactosidase activity when driven by a tissue-specific enhancer (28). We found DNaseI sensitivity in the proximal region of h923 (amplicon 4) in two independent primary keratinocyte samples, mirrored by genome-wide DNaseI hypersensitivity mapping in a proliferating human keratinocyte cell line (Fig. 5A, B and G; Crawford, personal communication). This finding was further corroborated by our observation of h923-*hsp68-lacZ* transgenic mice (F0) that demonstrated skin-specific β-galactosidase staining localized to the suprabasal layer of the epidermis (Fig. 5C). Consistent with the lack of luciferase activity under differentiating or proliferating conditions, we found no significant DNaseI sensitivity in h621 in two independent primary keratinocyte samples (genotyped as negative for the *LCE3C_LCE3B-del*) and in genome-wide DNaseI hypersensitivity mapping in a keratinocyte cell line (data not shown). However, h621-*hsp68-lacZ* transgenic mice (F0) demonstrated epidermal-specific *lacZ* expression at E16.5 that localized to the upper granular layer of the epidermis (Fig. 5D). Lack of enrichment for cells of the upper epidermal layers in primary tissue potentially contributes to our difficulty obtaining positive DNaseI sensitivity results for h621. Together, these results demonstrate *in vivo* epidermal-specific enhancer activities in h621 and h923. As well, this data suggests that the loss of enhancer function in the psoriasis-associated *LCE3C_LCE3B-del* (h621) may function as a contributing disease variant in psoriasis.

DISCUSSION

Our multidisciplinary study demonstrates a network of interspersed *cis*-regulatory elements in the EDC to coordinate gene expression during mammalian epidermal differentiation. Furthermore, we report a striking degree of synteny and linearity in EDC across eutherian and metatherian mammalian phylogenetic species. Discovery of extant metatherian evolutionary origins in the development of a unique mammalian tissue empowered our comparative genomics studies ascertaining CNEs as regulatory elements. We demonstrate the dynamic nature of regulatory activity of EDC CNEs with enhancer and repressor activity in differentiating versus proliferating conditions. Moreover, we show that two CNEs (h621 and h923) demonstrate *in vivo* epidermal-specific, developmental enhancer activity using DNaseI hypersensitivity assays and transgenic mice.

h923 enhancer is sufficient to direct epidermal tissue specificity

h923 demonstrated consistent high enhancer activity in our cell reporter assays suggesting a dual regulatory role in proliferating and differentiating conditions. Although h923 partially overlaps with a previously described distal regulatory region in the human *IVL* promoter required for tissue-specificity and expression when tested with its endogenous promoter in transgenic mice (29), our results demonstrate that h923 is sufficient to direct epidermal tissue specificity without its native *IVL* promoter.

h621 enhancer maps to the psoriasis-associated *LCE3C_LCE3B-del*

Despite our observation of negative cell-based reporter results in h621, we were able to demonstrate *in vivo* epidermal-specific enhancer activity in our transgenic mice. Our findings are consistent with previous reports of regulatory polymorphisms that fail to recapitulate their *in vivo* effects in cell-based assays (30). Identification of *in vivo* developmental enhancer activity in h621 mapping within the psoriasis-associated *LCE3C_LCE3B-del* allele suggests an alternative disease mechanism in *LCE3C_LCE3B-del*-psoriasis, a loss of regulatory activity affecting global transcription of the EDC.

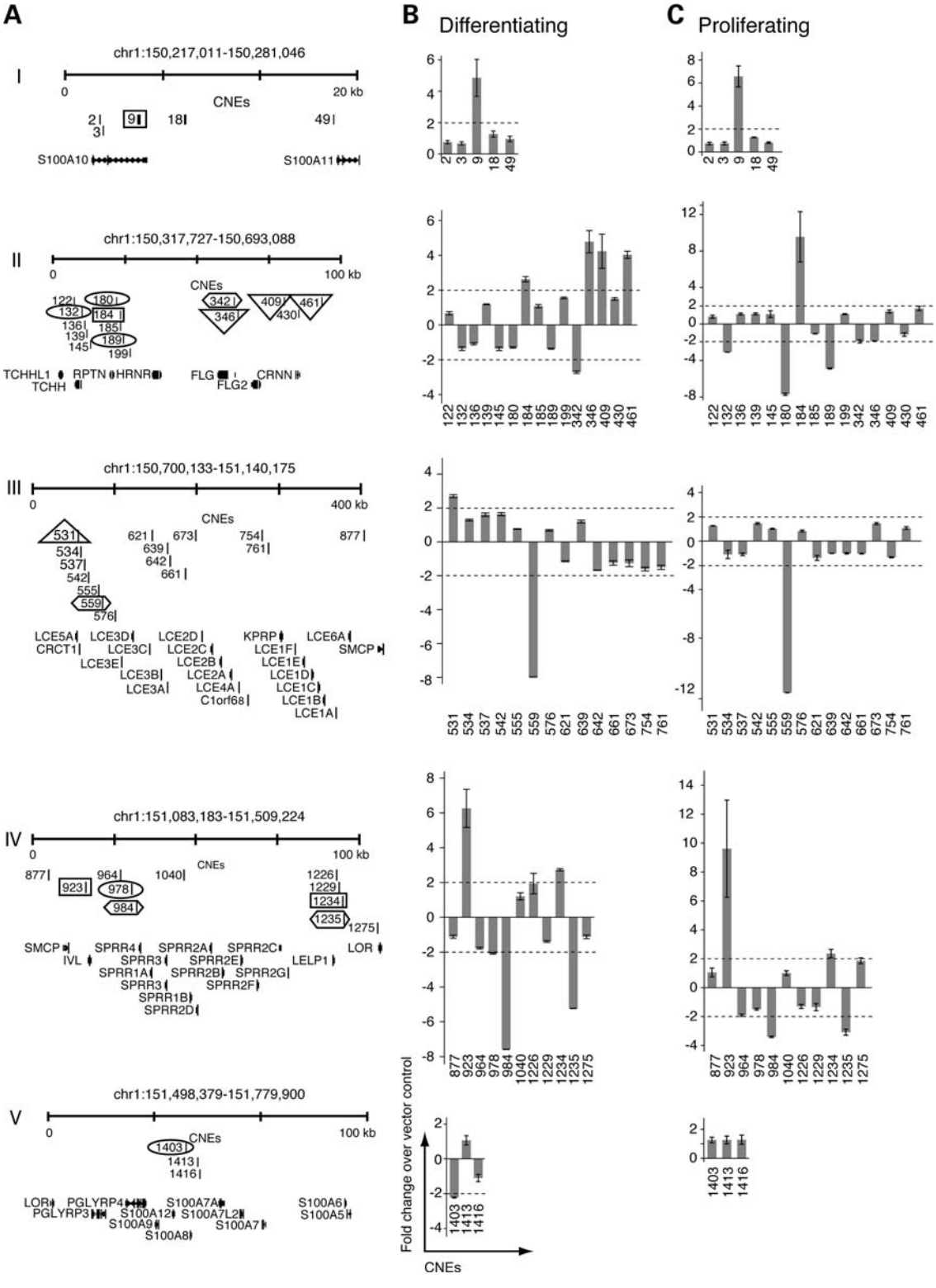

Figure 4. Regulatory activities in the CNEs of the EDC. (**A**) CNEs (grouped into clusters I–V, as depicted in Fig. 1) are labeled as distance (kb) from the *S100A10* transcriptional start site. Identification of CNEs span (hg18) chr1:150 202 011–151 891 137 including −20 kb of the transcriptional start site of *S100A10* and +20 kb downstream from *S100A1* transcript. EDC CNEs were tested for *in vitro* enhancer and repressor activity (luciferase reporter assays) in keratinocytes under (**B**) differentiating and (**C**) proliferating conditions. CNEs exhibiting >2-fold increased luciferase activity demonstrate enhancer activity and those that exhibit >2-fold decreased luciferase activity demonstrate repressor activity. Columns represent an average of two independent experiments performed in duplicate. Numbered CNEs are highlighted in designated boxes where Rectangle = enhancers (differentiating and proliferating), Hexagon = repressors (differentiating and proliferating), Triangle = enhancers (differentiating only), Oval = repressors (proliferating only), Bars, standard error.

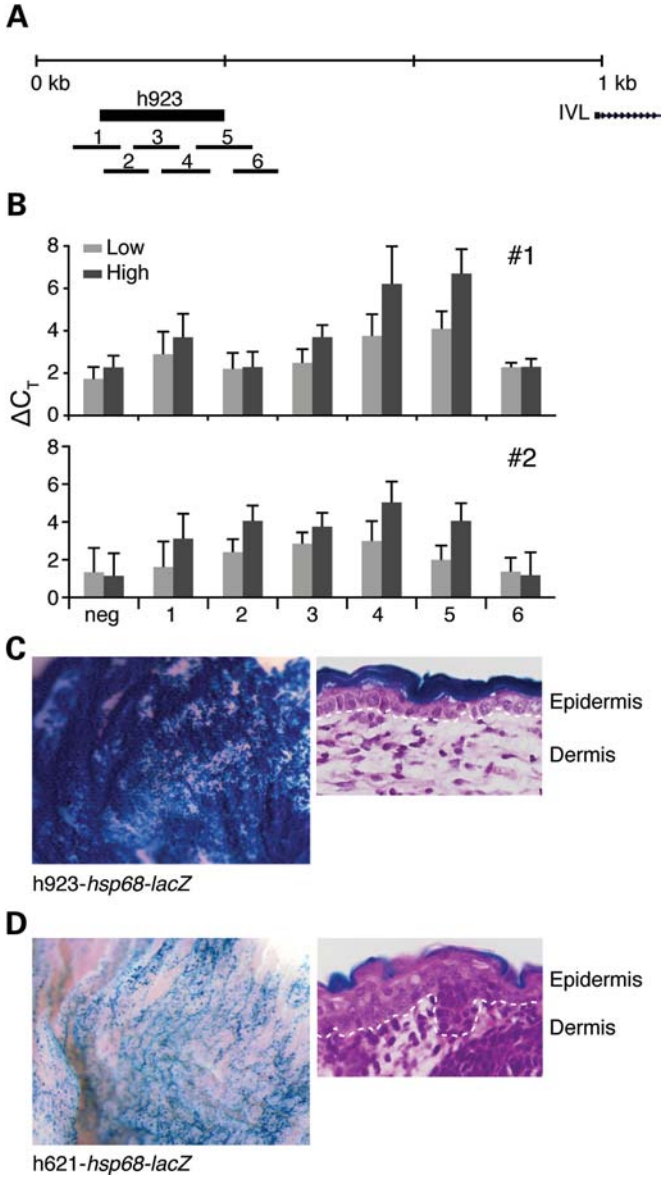

Figure 5. h923 and h621 in *LCE3C_LCE3B-del* function as enhancers *in vivo*. Enhancer activity was assayed by DNaseI hypersensitivity and transgenic *hsp68-lacZ* mice. (**A**) PCR amplicons of tiling primer sets (1–6) targeting h923 are indicated. (**B**) DNaseI sensitivity ($\Delta C_T = \Delta C_T$[DNase-treated] − ΔC_T[No DNase]) of individual primary keratinocyte samples (#1, #2) of h923. Light grey = low DNaseI, dark grey = hi DNaseI. Results are an average of triplicate readings. Bars, standard error. (**C**) h923-*hsp68-lacZ* transgenic mice (F0) demonstrate β-galactosidase-staining in the skin. All β-galactosidase-stained h923-*hsp68-lacZ* mice (two out of five genotyped-*lacZ*+ F0 mice) stained skin-specific at E16.5 (shown) and at pnd0. (**D**) h621-*hsp68-lacZ* (F0) demonstrate β-galactosidase-staining in the skin at E16.5. Five h621-*hsp68-lacZ* mice genotyped positive for *lacZ*. Four were β-galactosidase positive and two were skin-specific (shown). The remaining two β-galactosidase positive mice showed non-specific staining in the paws and brain (data not shown). H&E stains of β-galactosidase-stained cross-sections of the skin, Dotted lines indicate basement membrane demarcating the epidermis from the dermis, 40×.

Cluster of regulatory elements (Group II): association with AD?

Interestingly, the first genome-wide association study for AD recently identified a tagging SNP in linkage disequilibrium (LD) with the *FLG*-like gene family within the EDC even when excluding individuals with the two common mutations in the *FLG* locus (R501X and 2282del4) (9). Another study for AD also demonstrated linkage to the EDC even after excluding the FLG common mutations (31). Since these studies only genotyped subjects for the two common *FLG* mutations, it is possible that either other *FLG* variants or alternatively, other genetic variants within the LD block account for the residual association in these studies (12). To that end, we observe a cluster of CNEs with some of the highest regulatory activity under differentiating conditions in this LD block (Group II, Fig. 5A), suggesting possible *FLG*-like gene regulatory regions to analyze in AD etiology.

Developmental enhancers in disease

This study augments the evidence that developmental enhancers may be implicated and causative in disease (32). In addition to their role in development, they may also play an extensive role in regulating adult tissue repair and in the case of skin diseases, response to barrier impairment or environmental stress. As we learn more about the role of lincRNAs and miRNAs that are also evolutionarily conserved (33,34), it would be intriguing to investigate whether our CNEs encode these small RNA molecules as well. In summary, our study not only provides a much-anticipated source of potential genetic variants in AD and psoriasis but also underscores the importance of extensive genomic and complementary functional studies in conjunction with genetic studies.

MATERIALS AND METHODS

Semiquantitative real-time PCR

RNA was extracted from the dorsal skin of E13.5, E15.5 and E16.5 mice with TRIzol/chloroform (Invitrogen) and RNeasy purification (Qiagen). cDNA was generated from the RNA (5 μg) using Superscript VILO cDNA kit (Invitrogen). Semi-quantitative real-time PCR on cDNA was performed in triplicate (ABI 7300) using primers specific for target sequence (35) (Supplementary Material, Table S2) and SYBR Green (Invitrogen) to measure increased fluorescence of targeted amplicon. Primers used in this study amplify across intron boundaries where available and were confirmed for specificity using UCSC's 'in silico PCR' feature. Real-time PCR analysis (using the $\Delta\Delta C_T$ method per manufacturer's instructions) included experimental data with single-peak dissociation curves and normalization to β_2-microglobulin expression.

Comparative genomic sequence analysis

The EDC loci from human (hg18), chimp (panTro2), rhesus (rheMac2), mouse (mm8), rat (rn4), dog (canFam2) and opossum (monDom4) sequences were obtained from UCSC using the 'convert' option from the human reference sequence and aligned using Multispecies Percent Identity Plot Maker, MultiPipMaker (36) to obtain CNEs. 'Single coverage' and 'repeat masked sequence' options were selected in MultiPipMaker to exclude false positive regions that could be generated from paralogous gene sequences represented in the

EDC. Sequences identified by MultiPipMaker as alignable with at least 100 bp and >50% nucleotide identity across all seven mammalian genomes in non-coding regions were designated as CNEs. CNEs immediately adjacent to exon and introns were excluded. For synteny block analysis, the EDC loci were aligned using Mauve (version 2.3.0) (37) with the default settings and seed families enabled.

Luciferase assay

A library of CNE and NCNE from the EDC was generated by PCR amplification from human BAC clones using Fast Start Fidelity *Taq* (Roche) and subsequent cloning into Gateway (Invitrogen) compatible pGL3 (Promega) plasmids upstream of a mouse *Sprr1a* promoter driving firefly luciferase expression. NCNE were selected using a sliding window view of the human EDC locus to identify non-conserved (no shared alignment between mouse, rat, dog and opossum) DNA sequences across the EDC locus in intergenic regions that represented a range from 115 to 1109 bp and a median size of 496 bp similar to the CNEs. All CNEs and NCNEs were sequence verified. Dual luciferase assays (Promega) were performed in duplicate in two independent experiments on mouse SP-1 keratinocytes plated on 6-well plates under proliferating (0.05 mM Ca^{2+}) or terminal differentiating (1.3 mM Ca^{2+}) conditions in S-MEM/10% chelex-treated fetal bovine serum (Lifeblood Medical) and measured 24 and 72 h post-transfection (Fluorskan Ascent FL fluorimeter, Thermo Scientific), respectively (35). For each well, firefly luciferase activity was normalized to the co-transfected *Renilla* luciferase activity and empty vector control.

DNaseI hypersensitivity assay

Human skin samples were obtained with appropriate informed consent and reviewed by the NIH Office of Human Subject Review. Only human newborn foreskin samples that screened negative for the *LCE3C_LCE3B-del* (positive for LCE3CF/LCE3CR PCR allele and negative for the EDCDELL/EDCDELR PCR allele) (14) were analyzed for the h621 DNaseI assay. Foreskin samples were cut into 1 cm pieces and incubated on dispase:HBSS (1:1) (BD Biosciences) with dermis down at 4°C overnight. Epidermal sheets were peeled off the next day and incubated in 0.25% trypsin/EDTA at 37°C for 10′ with frequent shaking and pipetting to obtain single cell isolation. Single cells were lysed with 0.03% NP-40/10 mM Tris–HCl (pH 7.5)/10 mM NaCl/3 mM $MgCl_2$ buffer and digested with increasing amounts of DNaseI (Roche) at 37°C to obtain DNaseI-treated nuclei. After removal of proteins with overnight proteinase K digestion, DNaseI-digested DNA was subsequently isolated via phenol/chloroform extraction. Double-stranded DNA was quantitated using PicoGreen (Invitrogen) according to the manufacturer's instructions. DNaseI sensitivity was assayed by real-time PCR (ABI 7300) using 9.5 ng of DNaseI-digested DNA, SYBR Green (Qiagen) and tiling primers (200 bp amplicons with 50 bp overlap) to amplify targeted sequence (Supplementary Material, Table S3) (27). A non-conserved region (~8.7 kb downstream of *SPRR3*) was designed as a negative DNaseI control.

In vivo mouse enhancer assay

All animals were maintained in an AAALAC accredited, murine pathogen-free facility at the National Institutes of Health (Bethesda, MD, USA) in accordance with institutional protocols and the Guide for the Care and Use of Laboratory Animals. All animal procedures were approved by the NHGRI Animal Care and Use Committee. CNEs were cloned into the Gateway-compatible *hsp68-lacZ* reporter vector (gift from Marcelo Nobrega, University of Chicago), sequence-verified, purified by cesium chloride gradient (Loftstrand) and linearized with *Sal*I (NEB) prior to injection into fertilized eggs that were implanted into pseudopregnant females. Analysis was done on transgenic founder embryos (F0) at the corresponding embryonic stage post-transplantation (where transplantation day is designated as embryonic day [E] 0.5) and were genotyped using lacZ primers. Whole-mount embryos were stained overnight for β-galactosidase staining activity using X-gal (Fermentas) after cold fixation as previously described (38). β-galactosidase stained tissue sections were obtained from paraffin blocks (Histoserv).

SUPPLEMENTARY MATERIAL

Supplementary Material is available at *HMG* online.

ACKNOWLEDGEMENTS

We thank Cherry Yang, Yicong Liu and Roli Mandana for technical expertise, Carole Yee for primary keratinocyte samples, Peter Chines for primer tile design, Elsa Escobar and Laurentine Sop for mouse husbandry and Julia Fekecs for assistance in preparing the figures. We thank Greg Crawford and David Sankoff for helpful discussions with the genome-wide DNase hypersensitivity data and genomic synteny, respectively. We also thank Anne Bowcock, Elizabeth Grice and Stacie Loftus for manuscript critiques.

Conflict of Interest statement. None declared.

FUNDING

This work was supported by the National Human Genome Research Institute Intramural Research Program and the National Institute of Health K99AR055948 to C.G.S.

REFERENCES

1. Volz, A., Korge, B.P., Compton, J.G., Ziegler, A., Steinert, P.M. and Mischke, D. (1993) Physical mapping of a functional cluster of epidermal differentiation genes on chromosome 1q21. *Genomics*, **18**, 92–99.
2. Zhao, X.P. and Elder, J.T. (1997) Positional cloning of novel skin-specific genes from the human epidermal differentiation complex. *Genomics*, **45**, 250–258.
3. Mischke, D., Korge, B.P., Marenholz, I., Volz, A. and Ziegler, A. (1996) Genes encoding structural proteins of epidermal cornification and S100 calcium-binding proteins form a gene complex ('epidermal differentiation complex') on human chromosome 1q21. *J. Invest. Dermatol.*, **106**, 989–992.
4. Marshall, D., Hardman, M.J., Nield, K.M. and Byrne, C. (2001) Differentially expressed late constituents of the epidermal cornified envelope. *Proc. Natl. Acad. Sci. USA*, **98**, 13031–13036.

5. Eckert, R.L., Broome, A.M., Ruse, M., Robinson, N., Ryan, D. and Lee, K. (2004) S100 proteins in the epidermis. *J. Invest. Dermatol.*, **123**, 23–33.
6. Segre, J.A. (2006) Epidermal barrier formation and recovery in skin disorders. *J. Clin. Invest.*, **116**, 1150–1158.
7. Cookson, W.O., Ubhi, B., Lawrence, R., Abecasis, G.R., Walley, A.J., Cox, H.E., Coleman, R., Leaves, N.I., Trembath, R.C., Moffatt, M.F. *et al.* (2001) Genetic linkage of childhood atopic dermatitis to psoriasis susceptibility loci. *Nat. Genet.*, **27**, 372–373.
8. Palmer, C.N., Irvine, A.D., Terron-Kwiatkowski, A., Zhao, Y., Liao, H., Lee, S.P., Goudie, D.R., Sandilands, A., Campbell, L.E., Smith, F.J. *et al.* (2006) Common loss-of-function variants of the epidermal barrier protein filaggrin are a major predisposing factor for atopic dermatitis. *Nat. Genet.*, **38**, 441–446.
9. Esparza-Gordillo, J., Weidinger, S., Folster-Holst, R., Bauerfeind, A., Ruschendorf, F., Patone, G., Rohde, K., Marenholz, I., Schulz, F., Kerscher, T. *et al.* (2009) A common variant on chromosome 11q13 is associated with atopic dermatitis. *Nat. Genet.*, **41**, 596–601.
10. Smith, F.J., Irvine, A.D., Terron-Kwiatkowski, A., Sandilands, A., Campbell, L.E., Zhao, Y., Liao, H., Evans, A.T., Goudie, D.R., Lewis-Jones, S. *et al.* (2006) Loss-of-function mutations in the gene encoding filaggrin cause ichthyosis vulgaris. *Nat. Genet.*, **38**, 337–342.
11. Baurecht, H., Irvine, A.D., Novak, N., Illig, T., Buhler, B., Ring, J., Wagenpfeil, S. and Weidinger, S. (2007) Toward a major risk factor for atopic eczema: meta-analysis of filaggrin polymorphism data. *J. Allergy Clin. Immunol.*, **120**, 1406–1412.
12. Sandilands, A., Terron-Kwiatkowski, A., Hull, P.R., O'Regan, G.M., Clayton, T.H., Watson, R.M., Carrick, T., Evans, A.T., Liao, H., Zhao, Y. *et al.* (2007) Comprehensive analysis of the gene encoding filaggrin uncovers prevalent and rare mutations in ichthyosis vulgaris and atopic eczema. *Nat. Genet.*, **39**, 650–654.
13. Morar, N., Cookson, W.O., Harper, J.I. and Moffatt, M.F. (2007) Filaggrin mutations in children with severe atopic dermatitis. *J. Invest. Dermatol.*, **127**, 1667–1672.
14. de Cid, R., Riveira-Munoz, E., Zeeuwen, P.L., Robarge, J., Liao, W., Dannhauser, E.N., Giardina, E., Stuart, P.E., Nair, R., Helms, C. *et al.* (2009) Deletion of the late cornified envelope LCE3B and LCE3C genes as a susceptibility factor for psoriasis. *Nat. Genet.*, **41**, 211–215.
15. Zhang, X.J., Huang, W., Yang, S., Sun, L.D., Zhang, F.Y., Zhu, Q.X., Zhang, F.R., Zhang, C., Du, W.H., Pu, X.M. *et al.* (2009) Psoriasis genome-wide association study identifies susceptibility variants within LCE gene cluster at 1q21. *Nat. Genet.*, **41**, 205–210.
16. Visel, A., Bristow, J. and Pennacchio, L.A. (2007) Enhancer identification through comparative genomics. *Semin. Cell Dev. Biol.*, **18**, 140–152.
17. Blanpain, C. and Fuchs, E. (2009) Epidermal homeostasis: a balancing act of stem cells in the skin. *Nat. Rev. Mol. Cell. Biol.*, **10**, 207–217.
18. Jackson, B., Tilli, C.M., Hardman, M.J., Avilion, A.A., MacLeod, M.C., Ashcroft, G.S. and Byrne, C. (2005) Late cornified envelope family in differentiating epithelia–response to calcium and ultraviolet irradiation. *J. Invest. Dermatol.*, **124**, 1062–1070.
19. Cabral, A., Voskamp, P., Cleton-Jansen, A.M., South, A., Nizetic, D. and Backendorf, C. (2001) Structural organization and regulation of the small proline-rich family of cornified envelope precursors suggest a role in adaptive barrier function. *J. Biol. Chem.*, **276**, 19231–19237.
20. Margulies, E.H., Maduro, V.V., Thomas, P.J., Tomkins, J.P., Amemiya, C.T., Luo, M. and Green, E.D. (2005) Comparative sequencing provides insights about the structure and conservation of marsupial and monotreme genomes. *Proc. Natl. Acad. Sci. USA*, **102**, 3354–3359.
21. Mikkelsen, T.S., Wakefield, M.J., Aken, B., Amemiya, C.T., Chang, J.L., Duke, S., Garber, M., Gentles, A.J., Goodstadt, L., Heger, A. *et al.* (2007) Genome of the marsupial Monodelphis domestica reveals innovation in non-coding sequences. *Nature*, **447**, 167–177.
22. Samollow, P.B. (2008) The opossum genome: insights and opportunities from an alternative mammal. *Genome Res.*, **18**, 1199–1215.
23. Hardman, M.J., Sisi, P., Banbury, D.N. and Byrne, C. (1998) Patterned acquisition of skin barrier function during development. *Development*, **125**, 1541–1552.
24. Hardman, M.J., Moore, L., Ferguson, M.W. and Byrne, C. (1999) Barrier formation in the human fetus is patterned. *J. Invest. Dermatol.*, **113**, 1106–1113.
25. Gibbs, R.A., Rogers, J., Katze, M.G., Bumgarner, R., Weinstock, G.M., Mardis, E.R., Remington, K.A., Strausberg, R.L., Venter, J.C., Wilson, R.K. *et al.* (2007) Evolutionary and biomedical insights from the rhesus macaque genome. *Science*, **316**, 222–234.
26. Felsenfeld, G. and Groudine, M. (2003) Controlling the double helix. *Nature*, **421**, 448–453.
27. Crawford, G.E., Holt, I.E., Mullikin, J.C., Tai, D., Blakesley, R., Bouffard, G., Young, A., Masiello, C., Green, E.D., Wolfsberg, T.G. *et al.* (2004) Identifying gene regulatory elements by genome-wide recovery of DNase hypersensitive sites. *Proc. Natl. Acad. Sci. USA*, **101**, 992–997.
28. Kothary, R., Clapoff, S., Darling, S., Perry, M.D., Moran, L.A. and Rossant, J. (1989) Inducible expression of an hsp68-lacZ hybrid gene in transgenic mice. *Development*, **105**, 707–714.
29. Crish, J.F., Gopalakrishnan, R., Bone, F., Gilliam, A.C. and Eckert, R.L. (2006) The distal and proximal regulatory regions of the involucrin gene promoter have distinct functions and are required for in vivo involucrin expression. *J. Invest. Dermatol.*, **126**, 305–314.
30. Cirulli, E.T. and Goldstein, D.B. (2007) In vitro assays fail to predict in vivo effects of regulatory polymorphisms. *Hum. Mol. Genet.*, **16**, 1931–1939.
31. Morar, N., Edster, P., Street, T.L., Weidinger, S., Di, W., Dixon, A.L., Taylor, M., Holt, R., Broxholme, J., Kloop, N. *et al.* (2007) Positional cloning of susceptibility genes for atopic dermatitis in the epidermal differentiation complex. *J. Invest. Dermatol.*, **127**, 531.
32. Epstein, D.J. (2009) Cis-regulatory mutations in human disease. *Brief Funct. Genomic Proteomic.*, **8**, 310–316.
33. Guttman, M., Amit, I., Garber, M., French, C., Lin, M.F., Feldser, D., Huarte, M., Zuk, O., Carey, B.W., Cassady, J.P. *et al.* (2009) Chromatin signature reveals over a thousand highly conserved large non-coding RNAs in mammals. *Nature*, **458**, 223–227.
34. Bartel, D.P. (2004) MicroRNAs: genomics, biogenesis, mechanism, and function. *Cell*, **116**, 281–297.
35. Martin, N., Patel, S. and Segre, J.A. (2004) Long-range comparison of human and mouse Sprr loci to identify conserved noncoding sequences involved in coordinate regulation. *Genome Res.*, **14**, 2430–2438.
36. Schwartz, S., Zhang, Z., Frazer, K.A., Smit, A., Riemer, C., Bouck, J., Gibbs, R., Hardison, R. and Miller, W. (2000) PipMaker—a web server for aligning two genomic DNA sequences. *Genome Res.*, **10**, 577–586.
37. Darling, A.C., Mau, B., Blattner, F.R. and Perna, N.T. (2004) Mauve: multiple alignment of conserved genomic sequence with rearrangements. *Genome Res.*, **14**, 1394–1403.
38. Hou, L., Panthier, J.J. and Arnheiter, H. (2000) Signaling and transcriptional regulation in the neural crest-derived melanocyte lineage: interactions between KIT and MITF. *Development*, **127**, 5379–5389.

SUPPLEMENTAL METHOD

Barrier Function Assay

Opossums were bred and maintained at the University of Illinois, Urbana mouse facility. All animal procedures were approved by the University of Illinois, Urbana's Animal Care and Use Committee. Dye penetration assays on opossums were performed as previously described in mice (1).

1. de Guzman Strong, C., Wertz, P.W., Wang, C., Yang, F., Meltzer, P.S., Andl, T., Millar, S.E., Ho, I.C., Pai, S.Y. and Segre, J.A. (2006) Lipid defect underlies selective skin barrier impairment of an epidermal-specific deletion of Gata-3. *J. Cell Biol.*, **175**, 661-670.

Supplementary Table 1

Position/Name on EDC	UCSC Coordinates		Size of CNE
	Beginning	End	
2	150,223,484	150,223,754	270
3	150,224,212	150,224,384	172
9	150,231,146	150,231,790	644
18	150,240,740	150,241,236	496
49	150,270,919	150,271,046	127
122	150,344,161	150,344,569	408
132	150,354,421	150,355,824	1,403
136	150,358,367	150,358,482	115
139	150,361,533	150,361,782	249
145	150,367,081	150,367,582	501
180	150,402,310	150,403,002	692
184	150,407,000	150,407,429	429
185	150,407,932	150,408,136	204
189	150,411,850	150,412,078	228
199	150,420,493	150,420,708	215
342	150,564,100	150,564,694	594
346	150,568,287	150,568,542	255
409	150,631,961	150,632,622	661
430	150,652,291	150,652,619	328
461	150,683,210	150,683,588	378
531	150,753,354	150,753,714	360
534	150,756,606	150,756,846	240
537	150,759,864	150,760,135	271
542	150,764,576	150,764,798	222
555	150,777,079	150,777,205	126
559	150,781,626	150,781,965	339
576	150,797,668	150,797,910	242
621	150,843,202	150,843,535	333
639	150,861,064	150,861,488	424
642	150,865,005	150,865,380	375
661	150,883,425	150,884,534	1,109
673	150,895,340	150,895,715	375
754	150,976,553	150,977,133	580
761	150,983,327	150,984,045	718
877	151,099,712	151,100,212	500
923	151,145,042	151,145,699	657
964	151,185,995	151,186,382	387
978	151,199,941	151,200,157	216

984	151,206,141	151,206,503	362
1040	151,262,915	151,263,751	836
1226	151,448,012	151,448,260	248
1229	151,451,465	151,451,896	431
1234	151,455,875	151,456,726	851
1235	151,457,138	151,457,680	542
1275	151,497,219	151,497,516	297
1403	151,625,619	151,625,748	129
1413	151,635,685	151,635,943	258
1416	151,638,137	151,638,457	320

Supplementary Table 1. UCSC coordinates (hg18:chr1) of Epidermal Differentiation Complex Conserved Noncoding Elements defined by MultiPipMaker. Position on EDC reflects distance (kb) away from the *S100A10* transcriptional start site.

Supplementary Table 2

PCR	Forward Primer	Reverse Primer
S100a10	CTGAGAGTGCTCATGGAACG	TCCCCTTCTGCTTCATGTTT
S100a11	CCACCGTCAGCCACAGTC	ATCTAGCTGCCCGTCACAGT
Tchhl1	CACATTGCCCCACATTCC	CCCTCAAGGAGCTGTCTCAG
Rptn	CCTGCCTCTTCTGCTCATTC	CCGAAGGATGTCTCCAAACT
Horn	GCAAGCAACATCAGTCTCCA	CAGAATTTGGTGAAACTCTGTTACC
Flg	CTCCTTCAGCTGCATTCGAT	TGCCTGTAGTTGTCCTTCCA
Flg2	TGCGTCAGGCCTTATCCTAC	TCCTTCTCCAGCAGTTCCTT
Crnn	AACAGAAACTTGTCCCATCCTG	TGACGTCAGCAAACTCATGTT
Gm 4858	CTCAAGCATTCCACTCTCTGG	CCCCCAAATTCAGTGTAAATG
Lce1m	GCTGAGTGATCTACTCCAGTGC	GAGAGAGAATCGGGGCTTGT
Crct1	TTCTGCCTAGCAGGTGTCAA	AGCAAGAGGAGGAGGAGGAC
Lce3f	GCCTTCTTCTCCTACCTTTGC	CCAGAGCTTGTAGCACAGCA
Lce3c	TCTTCTCCTGCCTTTGCTGT	TGCTGATTCCTCCAGACTGT
Lce3b	AGCATCCTCAGACACGGACT	TGTAGCACAGCAGGAAGAGG
Lce3a	AAGTCTCCTATCACCTTCCCATC	AGCTTGTAGCACAGCACGAA
Lce1l	AGTTTCAGGCCCTGCTTCTT	CCAGGCTACAGCAGGAAGAC
Kprp	GCTCAGGTCCCAATCCAGTA	CCTTGGTCTCCACAACCACT
Lce1i	CAGATCTTGTGCTACCCTTCA	AATGGGCATTGTCGTTTCAT
Lce1h	TCCATTCACTGGCTGACTGA	TCCTGCACCATTTGTTTGAA
Lce1g	CACTGGCTGAGATACCCACA	CCACTGCTACAGCATCCAGA
Lce1f	ATCCACGCCATTAACACTGA	CCAGGCTACAGCAGGAAGAC
Lce1e	CCACTCACTGGGTGAGATACC	AACCCAAGCTACAGCAGGAA
Lce1d	ACTTCTCCTGAGGCGTCCAC	CCAGGCTACAGCAGGAAGAC
Lce1c	ACTGGCTGAGAAACCCACAG	CCAGGCTACAGCAGGAAGAC
Lce1a2	GCCCAAGGATCTTGTACTGC	CCAGGCTACAGCAGGAAGAC
Lce1b	TCCTCCTGAAGTGGCTACAGA	CCAGGCTACAGCAGGAAGAC
Lce1a1	CTCACCTTCCGAGGTATCCA	AAGACACAGGGGGACACTTG
Smcp	TCTGCTGAAACATCCAGGAA	GGATTTGGGACAGCAAGGT
Ivl	GCCTTCTCCCTCCTGTGAGT	ATGTTTGGGAAAGCCCTTCT
Sprr2b	TTCCTGGTACTCAAGCATTGG	CTTGGGTGGACACTTCTGCT
Prr9	TCCACATCCTTCATTGAATCTC	TTGGCTTAACTCCTGGCACT
Pglyrp3	TTGGCTTCTTGGCTCTCAGT	CAATGTCACACCAGCCTTTG
9130204L05Rik	ACACTCTGGGTGGCTCTTCTC	TTGGAAATTCACTTCTCACCAA
Pglyrp4	ATGCTGTCCTGGCTTCTTGT	TCAGCTTAGAGCTGCAACCA
S100a9	GAAGGAAGGACACCCTGACA	TCAACTTTGCCATCAGCATC
S100a8	CTGAGTGTCCTCAGTTTGTGC	GACCTGAGATATGATGACTTTATTCTG
S100a7a	GGATAGTGTGCCTCGCTTCA	AGACTGCCTGTCCTCCCTCT
S100a6	ATCCCCTCGACCACTCCTT	AGATCATCCATCAGCCTTGC
S100a5	GAGAAGGCACTGACCACCAT	CAATCTCCTGGTCGCTGTTT
S100a4	CCCAAACCTCTCTATTCAGCA	CTTTTCCCCAGGAAGCTAGG
S100a3b	AGCGTCTCCCTAGGTGCTG	GTCACACTCCCGGAACTCAC
S100a3a	AGGGACACCCAGTTGGTAGG	GCAGCTCCTTCTGCAACAAC
S100a16b	GTGTCCAGAGGCCCAGAGT	CGTCAGCATGTGGTTCAACT
S100a16a	GAGGAGGTGGACTCACAGGA	TCCAGGTTCTGGATGAGCTT
S100a14	GGCAGGCTATAGGACAGACG	CCTCAGCTCCGAGTAACAGG

S100a13	CCTTGCCTGGTGCTTATAAACTT	CCCTGCAAAGGTGAAGAAAG
S100a1	CAGTGGCCACATTTGCAG	TTCAGTTCTTTCTTGCTCAGCTT
B_2m	TGGTGCTTGTCTCACTGACC	CCGTTCTTCAGCATTTGGAT

Supplementary Table 2. Real-time Primers for Mouse Epidermal Differentiation Complex genes.

Supplementary Table 3

DNase Region	Forward	Reverse
neg	CTTCTTGCATCTGTGGTGGA	ACCCTGCTGCCATATTGTGT
h923-1	GGCATGGCTATTCAAGATGAG	CTAAGGATGCACTGGCTATTTC
h923-2	GCTCAAATAGGTTGCCTCACTC	GGGAGAGGTTCTTTCACTGC
h923-3	GGTGGGGGTTGGACAGTTA	AAAGCTAGGGTGTGGGAAAGA
h923-4	CCCTAGAATGTTGAGGTTTCC	AGTCAGTCTGGGGCAGCA
h923-5	GATACTGAGCCCCTGCTAACC	CAGTGCTATCCCCTCCTCAT
h923-6	CCCCAGAAAATGGCACAGT	CTGATTCCCCATAGTTTTCCTG
h621-1	GAGTCATTGATGCTTTCTGAGATT	CAGCTGCCAGTGGGTAAACT
h621-2	CACAGGTGCTATCTCTTCCAC	ATGAGGGACACCAGGGAGAC

Supplementary Table 3. Tiling Primers for DNaseI Regions.

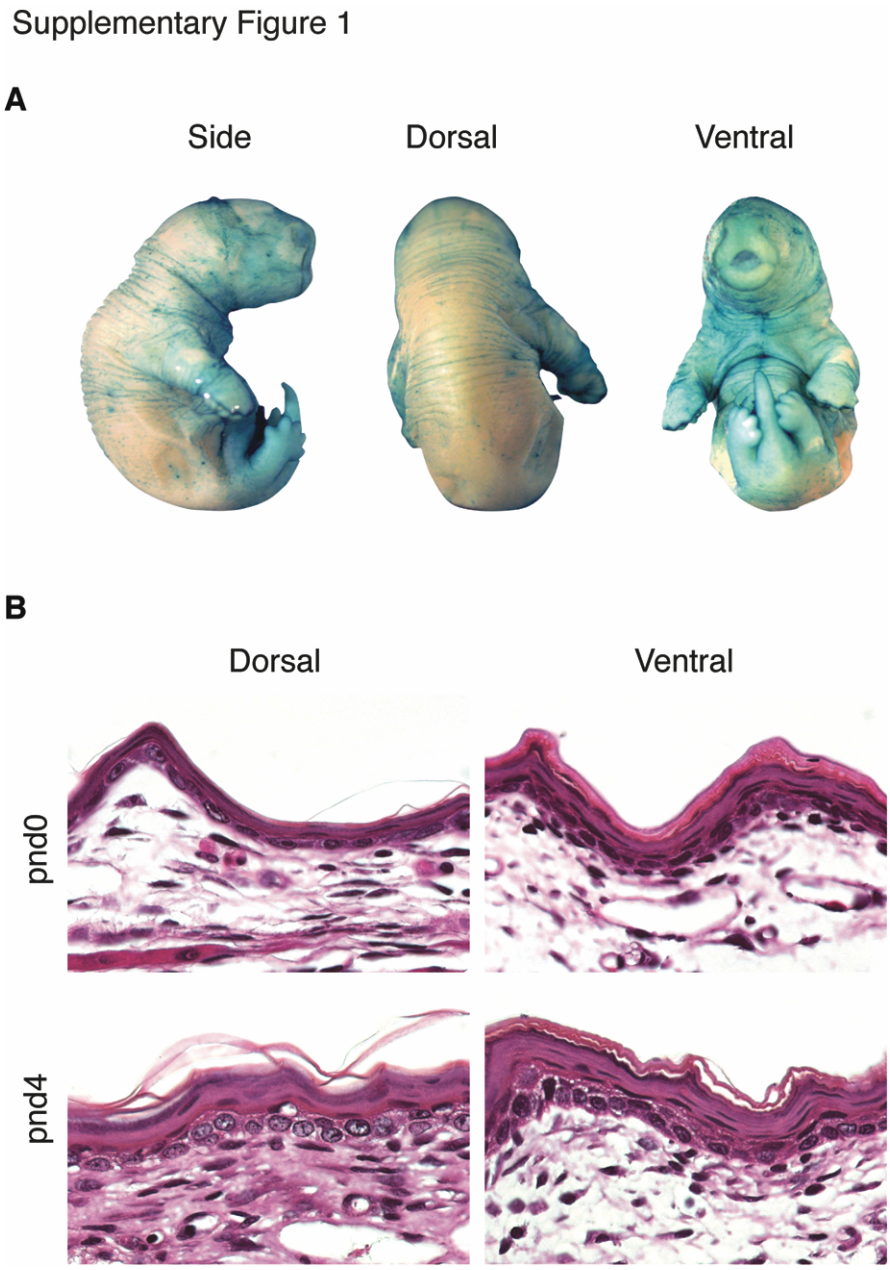

Supplementary Figure 1. Patterning of epidermal barrier formation is conserved to the metatherian opossum. (A) Dye exclusion assay of newborn opossum demonstrates patterning of epidermal barrier formation (dorsal to ventral migration). **(B)** Histology (dorsal and ventral) of the opossum at postnatal day (pnd) 0 (newborn) and pnd4, 40X magnification.